DOI: 10.1002/ejic.201000029

Photoactive Ternary Lanthanide-Centered Hybrids with Schiff-Base Functionalized Polysilsesquioxane Bridges and N-Heterocyclic Ligands

Jin-Liang Liu,[a] Bing Yan,*[a] and Lei Guo[a]

Keywords: Organic–inorganic hybrid composites / Lanthanides / Schiff bases / Luminescence / Polysilsesquioxane bridges

This work focuses on the synthesis of a series of silica-based organic–inorganic hybrid materials, containing different Schiff-base organic compounds, through a covalent self-assembly process. We first prepared three functional molecular bridges that can both coordinate to lanthanide ions (Eu^{3+} and Tb^{3+}) and form inorganic Si–O–Si networks with tetraethoxysilane (TEOS) from cohydrolysis and copolycondensation processes. Meanwhile, we selected N-heterocyclic ligands [1,10-phenanthroline (Phen) and 2,2′-bipyridine (Bipy)] as the second ligands to act as the main energy donor to absorb abundant energy in the UV/Vis region and to transfer the energy to the corresponding lanthanide ions to sensitize their emission. The introduction of the second ligand can also take the place of the coordinated H_2O and thus reduce the quenching effect of the OH group. Measurements of the photoluminescent properties of these materials show that the ternary lanthanide/inorganic/organic hybrids present stronger luminescent intensities and higher emission quantum efficiencies. The resulting amorphous materials exhibit regular, uniform microstructures and no phase separation occured since the organic and inorganic compounds were covalently linked through Si–O bonds through a self-assembly process.

Introduction

Because of their unique photophysical properties, lanthanide ions are well known as important components in photonics, especially with regard to their application in phosphors, lasers, and optical amplifiers.[1] The interesting chemical and photophysical properties of the Ln^{3+} ions are mostly attributed to the shielding of the 4f electrons from interactions with their surroundings by the filled $5s^2$ and $5p^6$ orbitals.[2] However, the direct Ln^{3+} photoexcitation is not very efficient, with the low molar absorption coefficients limiting the light output. Organic chelates are well known to be efficient sensitizers for the luminescence of lanthanide ions. These organic chromophores typically present effective absorption and a much broader spectral range than the corresponding Ln^{3+} ions and the energy they absorb can be transferred to nearby Ln^{3+} ions by an effective intramolecular-energy-transfer process. This process is called lanthanide luminescence sensitization or antenna effect.[3] Complexes of Ln^{3+} with various organic molecules, such as aromatic carboxylic acids, β-diketonates, calixarenes, cryptands, and heterocyclic ligands, have been described in some recent studies.[4] These materials, emitting efficiently in the near-UV, visible, and NIR spectral regions, are of great interest for a wide range of photonic applications, such as tunable lasers, amplifiers for optical communications, components of the emitter layers in multilayer organic light-emitting diodes (OLEDs), light concentrators for photovoltaic devices, and so on.[5]

However, with regard to the technological applicability, the somewhat low thermal and photochemical stability, together with the poor mechanical properties of lanthanide complexes result in some disadvantages. In order to overcome these drawbacks lanthanide complexes have been encapsulated into polymers,[6] liquid crystals,[7] and sol–gel derived organic–inorganic hybrids (mostly siloxane-based ones). Organic–inorganic hybrid materials have been developed over the past two decades affording materials with desired properties, since they combine some advantages of organic compounds (easy processing with conventional techniques, elasticity and organic functionalities) with properties of inorganic oxides (hardness, thermal and chemical stability, transparency), and thus have attracted considerable attention.[8] The sol–gel route is the most commonly employed method for the preparation of organic–inorganic hybrids at the macro/micro-scale, as well as at the molecular level under mild conditions. Moreover, by modifying the sol–gel processing conditions the microstructure, the external shape, or the degree of combination between the organic and the inorganic phases can be further controlled.[9]

Organic–inorganic hybrids can be classified according to the interaction established between the organic and inorganic components:[10] the physically doping hybrids and chemically bonding one. Carlos et al. have done important work and have recently written a review on the lanthanide-containing light-emitting organic–inorganic hybrids.[11] Binnemans has provided a more extensive and more recent

[a] Department of Chemistry, Tongji University,
Siping Road 1239, Shanghai 200092, P. R. China
Fax: +86-21-65982287
E-mail: byan@tongji.edu.cn

Supporting information for this article is available on the WWW under http://dx.doi.org/10.1002/ejic.201000029.

overview of the different types of lanthanide-based hybrid materials and compared their respective advantages and disadvantages.[12] Our research team has done extensive work where we have concentrated on covalently grafting the ligands to the inorganic networks in which the luminescent centers of the lanthanide complexes are bonded with a siloxane matrix through Si–O linkages. We have successfully realized six paths to construct the functional silylated precursors. In addition, after the modification, we assembled the above modified bridge ligands with lanthanide ions and tetraethoxysilane (TEOS) to compose hybrid systems with covalent bonds and obtained a series of stable and efficient molecular hybrid materials for use in optical areas.[13]

On the basis of former work, in this paper we synthesize three kinds of Schiff-base compounds (denoted as *o*-BASB, *p*-BASB, and *m*-BASB) containing a hydroxy group and a carboxyl group. The hydrogen-transfer nucleophilic addition reaction takes place between the hydroxy group and 3-(triethoxysilyl)propyl isocyanate (TESPIC) to achieve the molecular precursor (*o*-BASB-Si, *p*-BASB-Si, and *m*-BASB-Si), and the lanthanide ions (Eu^{3+} and Tb^{3+}) are coordinated through the carboxyl groups. A series of chemically bonded lanthanide/inorganic/organic hybrid materials (*o*-BASB-Si-Ln-Phen, *o*-BASB-Si-Ln-Bipy, *p*-BASB-Si-Ln-Phen, *p*-BASB-Si-Ln-Bipy, *m*-BASB-Si-Ln-Phen, and *m*-BASB-Si-Ln-Bipy, Ln = Eu or Tb) were thus constructed. Their physical characterization and photophysical properties are reported in detail.

Results and Discussion

1 Spectra Analyses for the Intermediate Product, the Silylated Precursors, and the Hybrid Materials

1.1 Nuclear Magnetic Resonance (NMR) Spectroscopy Analysis

The ^1H NMR spectroscopic data, relative to the organic compound BFPP, the Schiff-base compounds (*o*-BASB, *p*-BASB, and *m*-BASB), and the silylated precursors (*o*-BASB-Si, *p*-BASB-Si, and *m*-BASB-Si), are in full agreement with the proposed structures. The ^1H NMR chemical shifts from the OH bond are observed at around 3.20 ppm in the Schiff-base compounds (*o*-BASB, *p*-BASB, and *m*-BASB) and have disappeared in the corresponding silylated precursors (*o*-BASB-Si, *p*-BASB-Si, and *m*-BASB-Si), which indicate the accomplishment of the hydrogen-transfer reaction between –OH and TESPIC. The signal observed for the amino group –CONH– further confirms the grafting reaction. Furthermore, integration of the ^1H NMR signal corresponding to the ethoxy group shows that no hydrolysis of the precursor occurred during the grafting reaction.

1.2 FTIR Spectra

The synthesis of the intermediate product, BFPP, the Schiff-base compounds (*o*-BASB-Si, *p*-BASB-Si, and *m*-BASB-Si), and the grafting reaction of the Schiff-base compounds with TESPIC can also be confirmed by the FTIR spectra. Figure S2 (I) shows the IR spectra of BFPP (A), *o*-aminobenzoic acid (B), TESPIC (C), *o*-BASB (D), and *o*-BASB-Si (E) in the 4000–400 cm^{-1} range. The emergence of the strong vibration bond of OH at 3466 cm^{-1}, together with the characteristic absorption peaks of the Ar–O–CH_2 group located at around 1240, 1035 cm^{-1}, proves the formation of the organic compound BFPP.[14] The apparent characteristic absorption peak at 3471, 3374 cm^{-1} of amino groups is not observed in the IR spectrum of TESPIC. This, together with the emergence of the strong vibration bonds of C=N at around 1623 cm^{-1}, proves the formation of the Schiff-base compound *o*-BASB. The presence of a series of strong bands at 2975, 2928, 2886 cm^{-1} from the vibrations of methylene –$(CH_2)_3$– and the disappearance of the stretch vibration of the absorption peaks at 2277 cm^{-1} for N=C=O of TESPIC indicate that *o*-BASB has successfully been grafted onto TESPIC. The stretching vibration of Si–C located at about 1200 cm^{-1} and the stretching vibration of Si–O at 1107 cm^{-1} and 1077 cm^{-1}, together with the bending vibration at 460 cm^{-1}, indicate the absorption of the siloxane bonds. The *p*-BASB-Si and *m*-BASB-Si systems present similar features to those of the *o*-BASB-Si system.

All of the obtained hybrid materials were also characterized by infrared spectroscopy and they show similar features. The IR spectra of *o*-BASB-Si-Eu-Phen (a), *o*-BASB-Si-Eu-Bipy (b), *o*-BASB-Si-Tb-Phen (c), and *o*-BASB-Si-Tb-Bipy (d) are shown in Figure S1 (II). The broad absorptions of the ν(Si–C) vibration, which are located in the 1200–1192 cm^{-1} wavelength range, and the [ν(Si–O–Si)] vibration, which are located in the 1109–1060 cm^{-1} wavelength range can be seen in all of the spectra. The presence of the ν(Si–C) absorption is consistent with the fact that no (Si–C) bond cleavage occurs, while the absorption of ν(Si–O–Si) indicates the formation of siloxane bonds during the hydrolysis/condensation reactions. However, in the spectra, the ν(O–H) vibration at around 3400 cm^{-1} can also be observed, which confirms the existence of residual silanol groups and the presence of H_2O molecules. The ν(Si–OH) stretching vibration at 956 cm^{-1} is further evidence of the incompleteness of the condensation reactions. Furthermore, the complexation of Ln^{3+} with the organic compound in all of the hybrids can also be shown by infrared spectroscopy. Compared with the silylated precursor *o*-BASB-Si, the ν(COOH) vibrations at about 1684 cm^{-1} become very weak, while the $\nu_{as}(COO^-)$ and the $\nu_s(COO^-)$ vibrations located at 1592 and 1389 cm^{-1}, respectively, become much stronger. This is ascribed to the complexation of the Ln^{3+} ion with the oxygen atom of the COO^- group in the hybrids. The Ar–O–CH_2 vibrations in all of the hybrids are weakly shifted, which means that the oxygen atom of the Ar–O–CH_2 group does not take part in the complexation with the Ln^{3+} ion. As we know, it is very difficult to prove the exact structure of these types of noncrystalline hybrid materials and it is barely possible to solve the coordination behavior of lanthanide ions. But their main composition and coordination effect can be predicted according to the lanthanide coordination chemistry principle and the functional groups of the organic unit. The hybrid BASB-Si-Eu-Phen structure,

shown in Figure S1, was predicted from infrared spectroscopy and other previously reported references.[15] However, the presence of residual Si–OH groups in the complexes cannot be excluded. Similar features are observed for the *p*-BASB-Si and *m*-BASB-Si hybrids.

1.3 Powder XRD Spectra

The room-temperature X-ray diffraction patterns (determined from 10 to 70°) of the hybrid materials *o*-BASB-Si hybrids, *o*-BASB-Si-Eu-Phen, *o*-BASB-Si-Eu-Bipy, *p*-BASB-Si-Eu hybrids, *p*-BASB-Si-Tb-Phen, *p*-BASB-Si-Tb-Bipy, *m*-BASB-Si hybrids, *m*-BASB-Si-Eu-Phen, and *m*-BASB-Si-Tb-Bipy, reproduced in Figure S3, reveal that all the obtained hybrid materials are totally amorphous over a wide region. All the diffraction curves show similar broad peaks, with angle 2θ centered around 22°, which is characteristic of amorphous silica materials and are ascribed in the literature to encompass three distinct contributions in lamellar bridged silsesquioxanes.[16] The structural unit distance, calculated using the Bragg law, is approximately 4.11 Å. This may be ascribed to the coherent diffraction of the siliceous backbone of the hybrids.[17] The absence of any crystalline regions in these samples correlates with the presence of organic chains in the host inorganic framework.[18] In addition, none of the hybrid materials contain measurable amounts of phases corresponding to the pure organic compound or free Ln nitrate, which is an initial indication of the formation of the true covalent-bonded molecular hybrid material.

1.4 UV/Vis Diffuse Reflection Absorption Spectra

Diffuse reflectance experiments were performed on powdered materials for all of the materials. The corresponding diffuse reflection absorption spectra of *p*-BASB-Si-Eu hybrids, *p*-BASB-Si-Eu-Phen, *p*-BASB-Si-Tb-Phen, *p*-BASB-Si-Tb-Bipy, and *p*-BASB-Si-Tb-Bipy are given in Figure S4. All of the spectra exhibit broad absorption bands in the UV/Vis range 200–500 nm. These absorption bands correspond to the transition from the ground state to the first excited state ($S_0 \rightarrow S_1$) of the organic ligands, including Phen, Bipy, and the organosilanes. They are more specifically attributed to the $\pi \rightarrow \pi^*$ transitions occurring in the Phen, Bipy conjugating units, and the aromatic groups of the organosilanes. For *p*-BASB-Si-Ln-Phen and *p*-BASB-Si-Ln-Bipy a blue shift of the absorbance edge is observed compared with the *p*-BASB-Si hybrids. The absorbance bands of *p*-BASB-Si-Ln-Phen and *p*-BASB-Si-Ln-Bipy are mainly located at about 200–400 nm, which partially overlaps with the fluorescence excitation spectra (wide bands at 325–364 nm in Figure 2). In terms of the above phenomena, it can primarily be predicted that after the addition of the Phen and Bipy complexes the extent to which the energy levels between the hybrid host and lanthanide ions match one another is more suited and appropriate for the organic fragments of the hybrid to absorb abundant energy in the UV/Vis region and transfer the energy to the corresponding lanthanide ions. The *o*-BASB-Si and *m*-BASB-Si hybrid systems present similar features to those of the *p*-BASB-Si hybrids.

2 Scanning Electron Micrographs

The scanning electron micrographs for the hybrid materials demonstrate that a homogeneous system was obtained. Figure 1 shows the selected micrographs for the *o*-BASB-Si hybrid (A), *o*-BASB-Si-Eu-Phen (B), *o*-BASB-Si-Eu-Bipy (C), *p*-BASB-Si-Tb-Phen (D), *m*-BASB-Si-Eu-Phen (E), and *m*-BASB-Si-Tb-Phen (F) hybrid materials. In most cases the surface morphology of materials is of great importance for many technical applications requiring well-defined surfaces or interfaces. From Figure 1 we can see that all the samples show a homogeneous system and that no phase separation could be observed. This may be because the covalent bonding (Si–O–Si) enhanced the miscibility of the organic compounds and the silica matrixes so that the inorganic and the organic phases together exhibit their distinct properties under monophasic conditions. The *o*-BASB-Si hybrids have large block-structure microstructures with smooth surfaces as observed in Figure 1 (A). However, the micromorphology of the hybrids containing the Phen-Ln or Bipy-Ln complexes seems to be quite different from that of the *o*-BASB-Si hybrids, which are composed of many regular and uniform microballoon sphere-like microstructures that are about 20–30 μm in size. The differences between the microstructures may be due to the addition of the Ln complexes. For the *o*-BASB-Si hybrids without the Ln com-

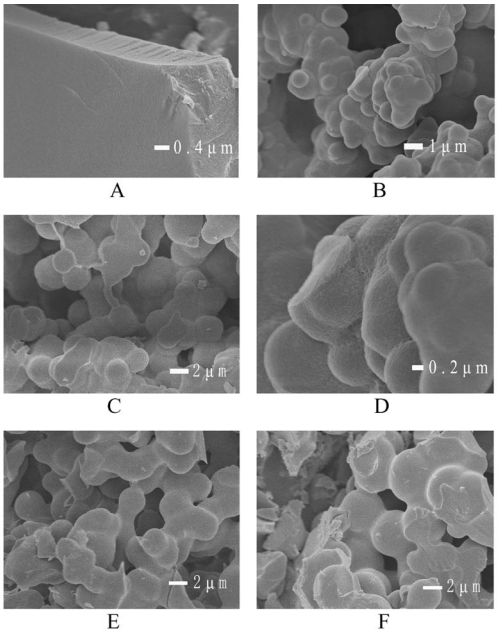

Figure 1. The selected SEM images for ternary lanthanide hybrid materials with organic and inorganic networks: *o*-BASB-Si hybrids (A), *o*-BASB-Si-Eu-Phen (B), *o*-BASB-Si-Eu-Bipy (C), *p*-BASB-Si-Tb-Phen (D), *m*-BASB-Si-Eu-Phen (E), and *m*-BASB-Si-Tb-Phen (F).

plexes the single hydrolysis and polycondensation reaction, which takes place between ethoxy–ethoxy, silanol–silanol, and ethoxy–silanol groups, occurs without any outer interaction disturbance. After the addition of the Phen-Ln or Bipy-Ln complex a more stable eightfold-coordinated structure with the Ln^{3+} ions is formed, which may readily provide orientation and induction ability. The hydrolysis and the polycondensation rate may decrease. Also, the organization may be induced under the chelation effect as well as other weak interactions such as van der Waals, London, and $\pi \rightarrow \pi$ stacking. In conclusion, the former only involves the sol–gel process (cohydrolysis and copolycondensation processes), while in the latter a strong coordination reaction occurs between the Ln^{3+} complexes and the BASB-Si host, which has a great influence on the sol–gel process and the microstructure or physical properties of the hybrids. This causes the large differences in the micromorphology of the hybrids.

3 Photoluminescence Properties of the Hybrid Materials

3.1 Photoluminescence Spectra

The binary lanthanide hybrids with Schiff-base functionalized polysilsesquioxane bridges show very weak (Figure S5) luminescence and only the $^5D_0 \rightarrow {}^7F_2$ transition of Eu^{3+} ($^5D_4 \rightarrow {}^7F_5$ transitions of Tb^{3+}) can be detected. On the basis of the enhancement of luminescent intensities of active lanthanide ions (such as Eu^{3+} and Tb^{3+}) by the addition of the second ligands in solution or solid complexes, we selected 2,2′-bipyridine and 1,10-phenanthroline as the second ligands to coordinate with the lanthanide ions in the cohybrid molecular materials. The introduction of the second ligand may take the place of the coordinated H_2O and thus reduce the quenching effect of the –OH group. In addition, the extent to which the energy levels between the organic segments and lanthanide ions match one another is more suited and appropriate as the second ligand, Phen or Bipy, becomes the main energy donor and thus reduces the nonradiative energy loss compared with the binary systems. Figure 2 shows the excitation and emission spectra of the europium hybrid materials (I) *p*-BASB-Si-Eu-Phen (A), *m*-BASB-Si-Eu-Phen (B), *p*-BASB-Si-Eu-Bipy (C), and *m*-BASB-Si-Eu-Bipy (D) and the terbium hybrid materials (II) *p*-BASB-Si-Tb-Phen (A), *o*-BASB-Si-Tb-Phen (B), *p*-BASB-Si-Tb-Bipy (C), and *m*-BASB-Si-Tb-Bipy (D). From the spectra we can see that the characteristic emissions of lanthanide ions are obtained, especially after the introduction of the second ligand Phen. The excitation spectra were obtained by monitoring the emission of Eu^{3+} or Tb^{3+} at 614 or 545 nm, respectively. For the Eu^{3+} hybrids, all the systems have similar excitation spectra that are dominated by a broad band from 325 to 364 nm with the maximum peak at about 345 nm. As a result the emission lines of the hybrid materials were assigned to the characteristic $^5D_0 \rightarrow {}^7F_j$ (J = 1, 2, 3, and 4) transitions at 590, 614, 650, and 685 nm, respectively. The $^5D_0 \rightarrow {}^7F_2$ emission around 614 nm is the most predominant transition. For the Tb^{3+} hybrids, a broad band centered at around 350 nm is observed in the excitation spectra and as a result the emission lines were assigned to the $^5D_4 \rightarrow {}^7F_j$ transitions located at 490, 544, 587, and 622 nm, for J = 6, 5, 4, and 3, respectively. The most striking green fluorescence ($^5D_4 \rightarrow {}^7F_5$) was observed because this emission is the most intense one. From the discussion on the photoluminescence spectra mentioned above we can see that the fluorescence intensities of molecular hybrids are much more enhanced when the second ligands are added to the hybrids, especially for the addition of 1,10-phenanthroline. This may be because the second ligand, Phen or Bipy, has become the main energy donor. It can absorb abundant energy in the UV/Vis region and transfer the energy to the corresponding lanthanide ions. So the problem of the Schiff-base compound not sensitizing the emission of the lanthanide ions was effectively avoided. Meanwhile, the steric effect of the Schiff-base com-

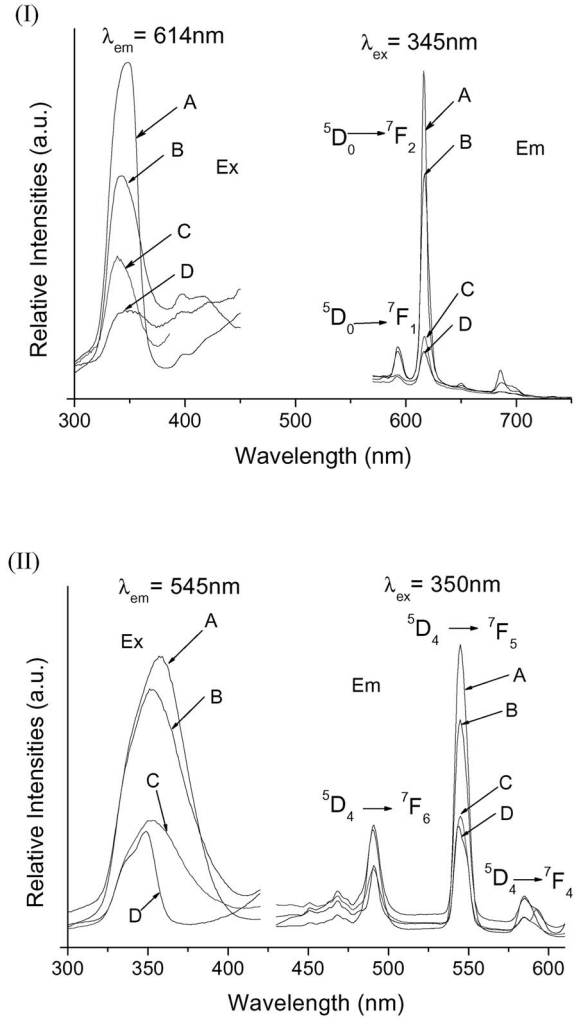

Figure 2. The selected excitation and emission spectra of the ternary europium hybrid materials (I): *p*-BASB-Si-Eu-Phen (A), *m*-BASB-Si-Eu-Phen (B), *p*-BASB-Si-Eu-Bipy (C), *m*-BASB-Si-Eu-Bipy (D) and the ternary terbium hybrid materials (II): *p*-BASB-Si-Tb-Phen (A), *o*-BASB-Si-Tb-Phen (B), *p*-BASB-Si-Tb-Bipy (C), *m*-BASB-Si-Tb-Bipy (D).

pound, which affects the coordination modality of Ln ions, can also have an influence on the fluorescence of the hybrids.

3.2 Luminescence Decay Times (τ) and Emission Quantum Efficiency (η) of the $^5D_0$ Excited State of the Europium Ion for the Eu^{3+} Hybrids

In order to further investigate the luminescence efficiency of these covalent hybrids, we selectively determined the emission quantum efficiencies of the excited state $^5D_0$ of the europium ion for the Eu^{3+} hybrids based on the emission spectra and lifetimes of the $^5D_0$ emitting level (Figure S6). Assuming that only nonradiative and radiative processes are essentially involved in the depopulation of the $^5D_0$ state, the quantum efficiency of the luminescence step, η, can be defined as how well the radiative processes compete with the nonradiative processes. The detailed principles and methods were adopted from ref.[19]

On the basis of the above discussion, we have determined the quantum efficiencies of the europium hybrid materials. As shown in Table 1, it can be seen that the value η mainly depends on the values of two quanta: one is the lifetime and the other is I_{02}/I_{01} (red/orange ratio). If the lifetimes and red/orange ratio are large the quantum efficiency must be high. The quantum efficiencies of the europium hybrid materials have been determined to follow the order: *p*-BASB-Si-Eu-Phen > *o*-BASB-Si-Eu-Phen > *m*-BASB-Si-Eu-Phen > *p*-BASB-Si-Eu-Bipy > *o*-BASB-Si-Eu-Bipy > *m*-BASB-Si-Eu-Bipy. The quantum efficiencies of *p*-BASB-Si-Eu-Phen (30.7%), *o*-BASB-Si-Eu-Phen (27.1%), and *m*-BASB-Si-Eu-Phen (23.4%) are much higher than those of *p*-BASB-Si-Eu-Bipy (10.0%), *o*-BASB-Si-Eu-Bipy (6.9%), and *m*-BASB-Si-Eu-Bipy (6.1%). So we can see that Phen is the better ligand for sensitizing the emission of the lanthanide ions. Furthermore, the quantum efficiencies of the BASB-Si-Eu-Phen hybrid systems are much higher than the hybrid materials with functional calix[4]arene organic ingredients (below 17%),[20] or those with functionalized thiosalicylic acids (below 21%)[21] from our previous work. This may be because the higher coordination atoms can be provided by these types of hybrids, and thus the more stable eightfold-coordinated structure with Ln^{3+} ions effectively reduces the quenching effect by the –OH group. The absolute luminescence quantum-efficiency data should be accurately obtained with an integrating sphere and a calibrated detector setup for solid materials.[11] In this article we only want to compare the photoluminescent behaviors of different hybrid materials, so the relative comparison using calculated values from lifetime and emission spectra is convenient and feasible. Certainly, the relative values of luminescent quantum efficiencies may be higher than the absolute values because they are only obtained from lifetime and spectrum data. Since the synthesis process can be easily applied to other organic ligands and to different alkoxysilanes we may be able to obtain stable and efficient hybrid materials for use in optical or electronic areas, because the desired properties can be tailored by an appropriate choice of the precursors and the addition of the second ligands.

Table 1. The luminescence efficiencies and lifetimes for the europium hybrids.

Hybrids	$A_{0-1,2}$ [s^{-1}]	A_{rad} [s^{-1}]	τ [μs][a]	η [%][b]
o-BASB-Si-Eu-Phen	50, 296	346	784	27.1
o-BASB-Si-Eu-Bipy	50, 148	198	351	7.0
p-BASB-Si-Eu-Phen	50, 306	356	864	30.7
p-BASB-Si-Eu-Bipy	50, 180	230	432	10.0
m-BASB-Si-Eu-Phen	50, 271	321	731	23.4
m-BASB-Si-Eu-Bipy	50, 135	185	329	6.1

[a] For the excited state $^5D_0$ of Eu^{3+}, whose error is ±50 μs. [b] For the $^5D_0$ quantum efficiency.

Conclusions

In summary, a series of lanthanide molecule-based hybrids containing organic Schiff-base compounds and inorganic networks (Si–O–Si) were assembled. Thanks to the addition of the second ligand of Phen and Bipy these hybrids present stronger luminescent intensities and a higher emission quantum efficiency, especially after the addition of Phen. This is a result of the second ligand acting as the main energy donor to absorb energy and to transfer the energy to the corresponding lanthanide ions through an intramolecular energy-transfer process. Uniform microstructures of these hybrids were also obtained where the organic and the inorganic compounds were covalently linked through Si–O bonds through a self-assembly process. The synthesis process can easily be applied to other organic ligands and to different alkoxysilanes and hence we may be able to obtain stable and efficient hybrid materials with the desired properties for use in optical or electronic areas.

Experimental Section

Physical Measurements: Fourier transform infrared (FTIR) spectra were measured within the 4000–400 cm^{-1} region with a Nicolet model 5SXC spectrophotometer using KBr disks. Nuclear magnetic resonance (NMR) spectra were recorded with a Bruker AVANCE-400 spectrometer with tetramethylsilane (TMS) as the internal reference. Scanning electron microscope (SEM) images were obtained with a Philips XL-30. The surface of the powdered sample was coated with gold before the measurement was taken. The X-ray diffraction (XRD) measurements were carried out with powdered samples with a Bruker D8 diffractometer (40 mA/40 kV) using monochromated Cu-$K_{\alpha 1}$ radiation (λ = 1.54 Å) over the 2θ range of 10° to 70°. Reflectivity spectra were recorded with a Bws003 spectrometer equipped with a diffuse reflectance accessory. Fluorescence excitation and emission spectra were obtained with an RF-5301 spectrophotometer with a 3 nm excitation slit and a 5 nm emission one. Luminescent lifetimes were recorded with an Edinburgh FLS 920 phosphorimeter using a 450 W xenon lamp as the excitation source (pulse width, 3 μs).

Chemicals: 3-(Triethoxysilyl)propyl isocyanate (TESPIC) was purchased from the Lancaster Company, other starting materials were purchased from Sinopharm Chemical Reagent Co., Ltd. (SCRC). Tetraethoxysilane (TEOS) was distilled and stored under a N_2 atmosphere. The solvents were purified according to literature procedures.[22] Europium and terbium nitrate were obtained by dissolving Eu_2O_3 and Tb_4O_7 in concentrated nitric acid, respectively. Other starting reagents were used as received.

Synthesis: The intermediate product 1,3-bis(2-formylphenoxy)-2-propanol (denoted as BFPP) was synthesized according to the procedure in ref.[23] The Schiff-base compounds (denoted as *o*-BASB, *p*-BASB, and *m*-BASB) and the corresponding silylated precursor (denoted as *o*-BASB-Si, *p*-BASB-Si, and *m*-BASB-Si) were prepared according to the procedure depicted in Figure S1 (I). The predicted structure of the hybrid *p*-BASB-Si-Ln-Phen, obtained from the co-condensation process between –OH groups of the silylated precursor BASB-Si and TEOS, is shown in Figure S1 (II).

Synthesis of Schiff-Base Compounds (*o*-BASB, *p*-BASB, and *m*-BASB): BFPP (1.501 g, 5.0 mmol) was dissolved in absolute ethanol (50 mL) and *o*-aminobenzoic acid (1.371 g 10 mmol) dissolved in absolute ethanol (50 mL) was then added dropwise. The resulting mixture was heated under reflux for about 8 h. After cooling, the solvent was removed in vacuo and the precipitate was filtered off. The crude product was purified by recrystallization from absolute ethanol and finally obtained as white crystals; yield 1.91 g (71.2%). ^{1}H NMR ($CDC1_3$, 400 MHz): δ = 3.22 (br., 1 H, OH), 4.24–4.62 (m, 5 H, CH_2CHCH_2), 6.98–8.01 (m, 16 H, ArH), 9.01 (s, 2 H, CH=N), 12.53 (s, 2 H, COOH) ppm.

p-BASB and *m*-BASB were prepared in a manner similar to the procedure described above for *o*-BASB. Recrystallization from absolute ethanol gave the desired products as white crystals. *p*-BASB: Yield = 78.2%. ^{1}H NMR ($CDC1_3$, 400 MHz): δ = 3.19 (br., 1 H, OH), 4.34–4.66 (m, 5 H, CH_2CHCH_2), 6.95–8.01 (m, 16 H, ArH), 8.93 (s, 2 H, CH=N), 12.63 (s, 2 H, COOH) ppm. *m*-BASB: Yield = 75.4%. ^{1}H NMR ($CDC1_3$, 400 MHz): δ = 3.26 (br., 1 H, OH), 4.20–4.59 (m, 5 H, CH_2CHCH_2), 6.93–8.01 (m, 16 H, ArH), 8.97 (s, 2 H, CH=N), 12.55 (s, 2 H, COOH) ppm.

Synthesis of Silylated Precursors (*o*-BASB-Si, *p*-BASB-Si, and *m*-BASB-Si): A typical synthetic procedure was as follows: The Schiff-base compound (1.0 mmol; *o*-BASB, *p*-BASB, or *m*-BASB) was dissolved in THF (10 mL). 3-(Triethoxysilyl)propyl isocyanate (denoted as TESPIC) (1.0 mmol) dissolved in THF (10 mL) was then added dropwise while stirring, and the mixture was kept at 60 °C overnight under argon in a covered flask. After cooling the solvent was removed in vacuo and the residue was washed three times with hexane (20 mL). A clear yellow oil was obtained. *o*-BASB-Si: ^{1}H NMR ($CDC1_3$, 400 MHz): δ = 0.61 (t, 2 H, CH_2Si), 1.02 (m, 2 H, $NHCH_2CH_2CH_2Si$), 1.24 (t, 9 H, CH_3CH_2), 2.58 (m, 2 H, $NHCH_2$), 3.81 (q, 6 H, $SiOCH_2$), 4.21–4.61 (m, 5 H, CH_2CHCH_2), 6.94–8.04 (m, 16 H, ArH), 7.42 (t, 1 H, NH), 9.03 (s, 2 H, CH=N), 12.74 (s, 2 H, COOH) ppm. *p*-BASB-Si: ^{1}H NMR ($CDC1_3$, 400 MHz): δ = 0.62 (t, 2 H, CH_2Si), 1.10 (m, 2 H, $NHCH_2CH_2CH_2Si$), 1.25 (t, 9 H, CH_3CH_2), 2.60 (m, 2 H, $NHCH_2$), 3.80 (q, 6 H, $SiOCH_2$), 4.04–4.52 (m, 5 H, CH_2CHCH_2), 6.88–8.11 (m, 16 H, ArH), 7.39 (t, 1 H, NH), 8.89 (s, 2 H, CH=N), 12.80 (s, 2 H, COOH) ppm. *m*-BASB-Si: ^{1}H NMR ($CDC1_3$, 400 MHz): δ = 0.61 (t, 2 H, CH_2Si), 1.12 (m, 2 H, $NHCH_2CH_2CH_2Si$), 1.23 (t, 9 H, CH_3CH_2), 2.68 (m, 2 H, $NHCH_2$), 3.80 (q, 6 H, $SiOCH_2$), 4.24–4.62 (m, 5 H, CH_2CHCH_2), 6.86–8.03 (m, 16 H, ArH), 7.52 (t, 1 H, NH), 8.91 (s, 2 H, CH=N), 12.73 (s, 2 H, COOH) ppm.

Synthesis of the Molecular Hybrid Materials Containing Lanthanide Ions (*o*-BASB-Si-Ln-Phen, *o*-BASB-Si-Ln-Bipy, *p*-BASB-Si-Ln-Phen, *p*-BASB-Si-Ln-Bipy, *m*-BASB-Si-Ln-Phen, and *m*-BASB-Si-Ln-Bipy, Ln = Eu^{3+} or Tb^{3+}): A typical procedure for the preparation of the hybrid materials was as follows: The precursor (*o*-BASB-Si, *p*-BASB-Si, and *m*-BASB-Si) and the second ligand (Bipy or Phen) were dissolved in a chloroform solution and a stoichiometric amount of $Ln(NO_3)\cdot 6H_2O$ was added. After 3 h, TEOS and H_2O were added while stirring, and then one drop of diluted hydrochloric acid was added to promote hydrolysis. The mmol ratio of $Ln(NO_3)\cdot 6H_2O$/BASB-Si/Bipy (or Phen)/TEOS/H_2O was 2:3:2:12:48. After the treatment of hydrolysis for 6 h an appropriate amount of hexamethylenetetramine was added to adjust the pH value to 6–7. The resulting mixture was agitated magnetically to achieve a single phase, and thermal treatment was performed at 60 °C in a covered Teflon® beaker for about 6 d until the sample solidified. The obtained gels were washed with ethanol and dried at 90 °C for another 2 d. The final molecular hybrid materials were collected as monolithic bulks and were ground into powdered materials for the photophysical studies. Free-Ln materials *o*-BASB-Si hybrids, *p*-BASB-Si hybrids, and *m*-BASB-Si hybrids were prepared in the same manner without the addition of the second ligand and $Ln(NO_3)\cdot 6H_2O$.

Supporting Information (see footnote on the first page of this article): Figures of the synthetic process, infrared spectra, X-ray diffraction graph of hybrid materials, UV/Vis diffuse reflection absorption spectra, and excitation and emission spectra of the binary lanthanide hybrid materials.

Acknowledgments

This work was supported by the National Natural Science Foundation of China (20971100) and Program for New Century Excellent Talents in University (NCET-08-0398).

[1] T. Justel, H. Nikol, C. Ronda, *Angew. Chem. Int. Ed.* **1998**, *37*, 3085–3103; K. Kuriki, Y. Koike, Y. Okamoto, *Chem. Rev.* **2002**, *102*, 2347–2356.
[2] N. Sabbatini, M. Guardigli, J. M. Lehn, *Coord. Chem. Rev.* **1993**, *123*, 201–228.
[3] J. M. Lehn, *Angew. Chem. Int. Ed. Engl.* **1990**, *29*, 1304–1319.
[4] B. Yan, H. J. Zhang, J. Z. Ni, *Mater. Sci. Eng.* **1998**, *B52*, 123–128; O. A. Serra, E. J. Nassar, I. L. V. Rosa, *J. Lumin.* **1997**, *72–74*, 263–266; K. Czarnobaj, M. Elbanowski, Z. Hnatejko, A. M. Klonkowski, M. Lis, M. Pietraszkiewicz, *Spectrochim. Acta Part A* **1998**, *54*, 2183–2187; M. Bredol, U. Kynast, M. Boldhaus, C. Lau, *Ber. Bunsen Ges. Phys. Chem.* **1998**, *102*, 1557–1560.
[5] J. Kido, Y. Okamoto, *Chem. Rev.* **2002**, *102*, 2357–2368; D. Parker, R. S. Dickins, H. Puschmann, C. Crossland, J. A. K. Howard, *Chem. Rev.* **2002**, *102*, 1977–2010; P. Gawryszewska, J. Sokolnicki, J. Legendziewicz, *Coord. Chem. Rev.* **2005**, *249*, 2489–2509; C. Adachi, M. A. Baldo, S. R. Forrest, *J. Appl. Phys.* **2000**, *87*, 8049–8055; B. G. Wybourne, *J. Alloys Compd.* **2004**, *380*, 96–100.
[6] V. Bekiari, P. Lianos, *Adv. Mater.* **1998**, *10*, 1455–1458; M. D. McGehee, T. Bergstedt, C. Zhang, A. P. Saab, M. B. O'Regan, G. C. Bazan, V. I. Srdanov, A. J. Heeger, *Adv. Mater.* **1999**, *11*, 1349–1354; V. D. Bermudez, L. D. Carlos, M. M. Silva, M. J. Smith, *J. Chem. Phys.* **2000**, *112*, 3293–3313.
[7] K. Binnemans, C. Görller-Walrand, *Chem. Rev.* **2002**, *102*, 2303–2345.
[8] T. Suratwala, Z. Gardlund, K. Davidson, D. R. Uhlmann, *Chem. Mater.* **1998**, *10*, 190–198; C. Molina, K. Dahmouche, C. V. Santilli, A. F. Craievich, S. J. L. Ribeiro, *Chem. Mater.* **2001**, *13*, 2818–2823.
[9] L. R. Matthews, E. T. Knobbe, *Chem. Mater.* **1993**, *5*, 1697–1701; B. Lebeau, C. E. Fowler, S. R. Hall, *J. Mater. Chem.* **1999**, *9*, 2279–2281; P. Innocenzi, H. Kozuka, T. J. Yoko, *J. Phys. Chem. B* **1997**, *101*, 2285–2291.
[10] C. Sanchez, F. Ribot, *New J. Chem.* **1994**, *18*, 1007–1037; H. R. Li, J. Lin, L. S. Fu, J. F. Guo, Q. G. Meng, F. Y. Liu, H. J. Zhang, *Microporous Mesoporous Mater.* **2002**, *55*, 103–107; K. Binnemans, P. Lenaerts, K. Driesen, C. Görller-Walrand, *J. Mater. Chem.* **2004**, *14*, 191–195; J. L. Liu, B. Yan, *J. Phys.*

Chem. C **2008**, *112*, 14168–14178; N. Lin, H. R. Li, Y. G. Wang, Y. Feng, D. S. Qin, Q. Y. Gan, S. D. Chen, *Eur. J. Inorg. Chem.* **2008**, 4781–4785.
[11] L. D. Carlos, R. A. S. Ferreira, V. D. Bermudez, J. L. S. Ribeiro, *Adv. Mater.* **2009**, *21*, 509–534.
[12] K. Binnemans, *Chem. Rev.* **2009**, *109*, 4283–4374.
[13] Q, M. Wang, B. Yan, *J. Mater. Chem.* **2004**, *14*, 2450–2455; L. Guo, B. Yan, *Eur. J. Inorg. Chem.* **2010**, 1267–1274; Q. M. Wang, B. Yan, *Cryst. Growth Des.* **2005**, *5*, 497–503; X. F. Qiao, B. Yan, *Inorg. Chem.* **2009**, *48*, 4714–4723; X. F. Qiao, B. Yan, *J. Phys. Chem. B* **2008**, *112*, 14742–14750; B. Yan, Q. M. Wang, *Cryst. Growth Des.* **2008**, *8*, 1484–1489.
[14] A. C. Franville, D. Zambon, R. Mahiou, S. Chou, Y. Troin, J. C. Cousseins, *J. Alloys Compd.* **1998**, *275–277*, 831–834; A. C. Franville, D. Zambon, R. Mahiou, *Chem. Mater.* **2000**, *12*, 428–435.
[15] H. S. Hoffmann, P. B. Staudt, T. M. H. Costa, C. C. Moro, E. V. Benvenutti, *Surf. Interface Anal.* **2002**, *33*, 631–634.
[16] L. D. Carlos, V. D. Bermudez, R. A. S. Ferreira, L. Marques, M. Assuncao, *Chem. Mater.* **1999**, *11*, 581–588; M. C. Goncalves, V. D. Bermudez, R. A. S. Ferreira, L. D. Carlos, D. J. Ostrovskii, J. Rocha, *Chem. Mater.* **2004**, *16*, 2530–2543; S. S. Nobre, C. D. S. Brites, R. A. S. Ferreira, V. D. Bermudez, C. Carcel, J. J. E. Moreau, J. Rocha, M. Wong Chi Man, L. D. Carlos, *J. Mater. Chem.* **2008**, *18*, 4172–4182.
[17] B. Yan, X. F. Qiao, *J. Phys. Chem. B* **2007**, *111*, 12362–12374.
[18] P. Tien, L. K. Chau, *Chem. Mater.* **1999**, *11*, 2141–2147.
[19] M. H. V. Werts, R. T. F. Jukes, J. W. Verhoeven, *Phys. Chem. Chem. Phys.* **2002**, *4*, 1542–1548; C. Y. Peng, H. J. Zhang, J. B. Yu, Q. G. Meng, L. S. Fu, H. R. Li, L. N. Sun, X. M. Guo, *J. Phys. Chem. B* **2005**, *109*, 15278–15287.
[20] H. F. Lu, B. Yan, J. L. Liu, *Inorg. Chem.* **2009**, *48*, 3966–3975.
[21] B. Yan, H. F. Lu, *Inorg. Chem.* **2008**, *47*, 5061–5611.
[22] D. D. Perrin, W. L. F. Armarego, D. R. Perrin, *Purification of Laboratory Chemicals*, Pergamon Press, Oxford, **1980**.
[23] J. L. Liu, B. Yan, *J. Phys. Chem. B* **2008**, *112*, 10898–10907.
Received: October 13, 2009
Published Online: April 13, 2010

